

1 **Community structure and feeding ecology of meiofauna associated with methane seepage**
2 **at the Darwin mud volcano (Gulf of Cádiz)**

3

4 Ellen Pape^{1,*}, Tania Nara Bezerra¹, Heleen Vanneste², Katja Heeschen², Leon Moodley³,
5 Frederic Leroux⁴, Peter van Breugel³ & Ann Vanreusel¹

6 ¹ Marine Biology Section, Biology department, Ghent University, Krijgslaan 281/S8, 9000
7 Gent, Belgium

8 ² National Oceanography Centre Southampton, University of Southampton, Waterfront
9 Campus, European Way, Southampton, SO14 3ZH UK

10 ³ NIOO-CEME, Workgroup of Ecosystem studies, Korringaweg 7, 4401 NT Yerseke, the
11 Netherlands

12 ⁴ EMAT, University of Antwerp, Groenenborgerlaan 171, B-2020 Antwerpen, Belgium

13 * Corresponding author, Ellen.Pape@Ugent.be

14 ABSTRACT: We sampled the Darwin mud volcano (MV) for meiofaunal community and
15 trophic structure in relation to pore-water geochemistry along a 10-m transect from a seep
16 site on the rim of the crater towards the MV slope. Pore-water profiles indicated
17 considerable variation in upward methane (CH₄) flow among sediment cores taken along the
18 transect, with highest flux in the seep sediment core, gradually decreasing along the
19 transect, to no CH₄ flux in the core taken at a 5 m distance. Low sulphate concentrations and
20 high levels of total alkalinity and sulphide (H₂S) suggested that anaerobic oxidation of
21 methane (AOM) occurred close to the sediment surface in the seep sediment core. High H₂S

22 levels had a genus and species-specific impact on meiofaunal densities. Nematode genus
23 composition varied gradually between sediment cores, with the genus *Sabatieria* dominating
24 almost all sediment cores. However, genus diversity increased with increasing distance from
25 the seep site. These limited data suggest that the community structure of seep meiofauna is
26 highly dependent on local (a)biotic habitat characteristics, and a typical seep meiofauna
27 community cannot be delineated. Stable isotope values suggested the nematode diet up to
28 10 m from the seep site included thiotrophic carbon. The thicker hemipelagic sediment layer
29 (photosynthetic carbon), the increased trophic diversity, and the heavier nematode $\delta^{13}\text{C}$
30 farther from the seep site suggest a decrease in thiotrophy and an increase in
31 photosynthetic carbon in the nematode diet.

32 Key words: cold seeps; diversity; stable isotopes; nematodes; diet

33

34

INTRODUCTION

35 Mud volcanoes (MVs), geological structures driven by fluid flow, are characterized by a high
36 patchiness of biochemical and physical characteristics. Fluid flow rates, pore-water
37 concentrations of hydrogen sulphide (H_2S) and methane (CH_4), and the thickness of the
38 hemipelagic sediment veneer, on top of the reduced sediments, can change rapidly over
39 short distances (m - cm) (Levin et al. 2003). The heterogeneity in these properties is the main
40 parameter driving the distribution of macro- and megafauna at seeps (Levin 2005), resulting
41 in patches of tubeworm clusters, mussels or clams, and bacterial mats or bare reduced
42 sediments. Meiofauna can also vary on a scale of meters in taxonomic composition and
43 biodiversity in relation to sediment biogeochemistry (Van Gaever et al. 2009c).

44 There is no consistent meiofaunal response to seep conditions. Meiofaunal densities
45 at different deep-sea seeps are higher (Olu-Le Roy et al. 1997, Van Gaever et al. 2006) or
46 similar (Shirayama & Ohta 1990) compared to non-seep sediments. In seep environments,
47 nematodes usually are the predominant metazoans, although sometimes copepods
48 dominate (Van Gaever et al. 2006). Generally, deep-sea nematodes are characterized by high
49 local diversity (Lamshead & Boucher 2003). Cold seeps, however, exhibit substantially
50 reduced species diversity, harbouring only a few dominant species (Levin 2005, Vanreusel et
51 al. 2010). The low diversity in these habitats has been attributed to the harsh abiotic
52 conditions, created by the high H₂S and low oxygen levels (Levin 2005).

53 Besides high biogeochemical and physical heterogeneity, seeps differ from most
54 deep-sea environments in the local production of organic matter through chemosynthesis.
55 Consequently, possible food sources for seep fauna, including meiobenthos, are (1) organic
56 matter derived from symbiotic chemoautotrophic bacteria, and (2) free-living
57 chemoautotrophic bacteria, in addition to (3) the photosynthetic organic matter, delivered
58 to all deep-sea habitats. Studies on the diet of seep meiofauna are few. Both Van Gaever *et*
59 *al.* (2006, 2009b) and Spies & DesMarais (1983) found seep nematodes to be feeding on
60 free-living sulphur-oxidising bacteria. To date, there is no evidence of symbioses between
61 nematodes and chemosynthetic bacteria at deep-sea seeps (Vanreusel et al. 2010), and
62 observations of symbionts associated with seep nematodes are restricted to shallow waters
63 (Dando et al. 1991, Ott et al. 2004).

64 This study examined the community structure and feeding ecology of the meiofauna,
65 with a focus on nematodes, at a MV in the Gulf of Cádiz, which we then related to
66 geochemical gradients along a 10-m transect going from a seep site towards nearby

67 hemipelagic surface sediments, and 2 sites farther away from seep influence. This study
68 differs from previous analyses on seep meiofauna, because it concerns isolated seep
69 sediments on a low-activity MV. We addressed the following questions:

- 70 - Does pore-water composition influence horizontal and vertical distribution of
71 meiofauna on a small scale?
- 72 - Are the seep sediments colonized by a specialized community that differs from the
73 hemipelagic sediments in density, biomass and taxonomic composition (genera and
74 species)?
- 75 - What is the nematode diet inferred from stable isotope analyses and buccal
76 morphology? Do seep conditions influence nematode trophic diversity?

77 MATERIALS AND METHODS

78 **Study area.** The Gulf of Cádiz (34°- 37°15' N, 9° - 6°45' W) is a tectonically active
79 region west of the Strait of Gibraltar, encompassing the boundary between the European
80 and African plate. It is one of the largest cold-seep areas on the European margins with over
81 30 MVs between 200 and 4000 m deep (Pinheiro et al. 2003, Somoza et al. 2003, Van
82 Rensbergen et al. 2005).

83 The summit (1100 m depth) of the Darwin MV (35°23.51' N 7°11.48'W; Fig. 1A) is
84 covered with a large, fractured carbonate crust. At the time of sampling, countless, but
85 mostly empty, *Bathymodiolus mauritanicus* shells covered the MV top (Genio et al. 2008).
86 Living specimens were only present in small clumps along cracks in the crust. When
87 disturbed by the ROV temperature probe, a small area of dark-coloured sediment (\pm 100
88 cm²), from here on referred to as “seep site”, emitted gas. Small carbonate blocks and white
89 sediments, indicative of bacterial activity, which covered hard substrate, surrounded the

90 seep site (Vanreusel et al. 2009). No dense aggregations of living chemosynthetic megafauna
91 were associated with the seep sediments or 2 m away. At the MV centre, non-
92 chemosynthetic megafauna comprised scavenging crabs, corals and stylasterine corals,
93 attached to the carbonate crust.

94 **Sampling strategy.** Sediment cores were collected during the JC10 expedition to the
95 Gulf of Cádiz in May 2007 onboard the RRS *James Cook* (Table 1). We were unable to collect
96 replicate samples because of the high heterogeneity of the habitat and the small size of the
97 seep site. However, this study is the first to identify potential interactions between seep
98 meiofauna and pore-water geochemistry measured at such a small spatial scale.
99 Furthermore, no meiofauna data were available from the Gulf of Cádiz so far, although it
100 forms an important faunal cross road between the Mediterranean and the Atlantic.

101 Using ROV Isis, we collected 2 push cores (PUCs, 25.5 cm²) at each of the 4 sites along
102 a 10-m transect between the seep site and an area with a considerably thicker hemipelagic
103 sediment layer (Fig. 1; Table 1). One PUC was taken with a core-liner, with openings every 2
104 cm, to extract pore-water using Rhizons (Seeberg-Elverfeldt et al. 2005). These pore-waters
105 were sub-sampled on board for nutrient and anion analyses. Subsequently, we sliced the top
106 10 cm of this core into 1-cm sections and fixed them in 4% formaldehyde for meiofaunal
107 community analysis. The 2nd PUC was sub-sampled for CH₄ and porosity analyses, and we
108 stored the remaining sediment in 2-cm slices at -30°C for stable isotope analysis. Besides the
109 10-m transect, we sampled 2 sites at ~ 100 (on the MV) and ~ 1100 m from the seep site (off
110 the MV) with a megacorer (75.4 cm²). These samples were exclusively analyzed for
111 community structure.

112 **Pore-water geochemical analyses.** Total alkalinity (TA) and hydrogen sulphide (H₂S)
113 were measured immediately after pore-water extraction; TA by titrating against 0.05 M HCl
114 while bubbling nitrogen through the sample (Ivanenkov & Lyakhin 1978) and H₂S using
115 standard photometric procedures (Grasshoff et al. 1999) adapted for pore-waters with high
116 (\cong mM) H₂S levels. Concentrations of all other species were analyzed at the National
117 Oceanography Centre Southampton (NOCS). Sulphate (SO₄²⁻) was measured by ion
118 chromatography (Dionex ICS2500), with reproducibility (determined by repeat analysis of a
119 seawater standard as well as single anion standards) >1.5%. We measured dissolved CH₄ in
120 sediment samples taken immediately after opening the cores using the headspace vial
121 method (Reeburgh 2007). An aliquot of sediment (\cong 3 cm³) was withdrawn, placed in a glass
122 vial, and 5 ml of 1M NaOH was added to prevent further microbial activity (Hoehler et al.
123 2000). The vial was crimped shut, and the sample shaken vigorously to release the gases.
124 CH₄ concentration in the headspace was determined by gas chromatography (Agilent 6850)
125 at the NOCS. These headspace CH₄ measurements were then converted to dissolved CH₄
126 concentrations following Hoehler et al. (2000). Depressurization and warming of the cores
127 during sediment retrieval is likely to have led to degassing, so concentrations of CH₄ (which is
128 generally oversaturated in pore-waters) and H₂S, to a lesser extent, represent minimum
129 values. Therefore, profiles were compared relative to one another, rather than to
130 measurements in other studies.

131 **Meiofaunal community analysis.** We washed the formaldehyde-fixed samples over a
132 32- μ m mesh sieve and extracted the meiofauna from the sediment by Ludox centrifugation
133 (Heip et al. 1985). Meiofauna was then sorted, enumerated and identified at coarse
134 taxonomic level. From each slice, \pm 100 nematodes were identified to genus level.
135 *Sabatieria*, the dominant genus in all cores but one, was identified to species. Additionally,

136 we measured length (μm) and maximal width (μm) for each nematode from the top 0-5 cm,
137 to estimate individual biomass using Andrassy's formula (Andrassy 1956) for wet body
138 weight (wwt), adjusted for the specific gravity of marine nematodes (i.e. 1.13 g cm^{-3} ; $\mu\text{g wwt}$
139 = $L \times W^2 / 1\,500\,000$). C weight was calculated as 12.4 % of wet weight (Jensen 1984).

140 **Stable isotope analysis.** Nematodes from the top 6 cm of each core were hand-
141 picked for $\delta^{13}\text{C}$ and $\delta^{15}\text{N}$ analysis. *Desmodora* ($n = 50$) and *Sabatieria* ($n = 50$) were picked
142 separately, and the remaining genera were pooled to determine the "Mix" isotope value ($n =$
143 100). When not sufficiently abundant, *Desmodora* and/or *Sabatieria* were included in the
144 "Mix" sample. Nematodes were rinsed with $2 \mu\text{m}$ filtered Milli-Q water, and then transferred
145 to Milli-Q water in pre-combusted (550°C , 3 h) silver cups. After elutriation, nematodes were
146 dried overnight at 60°C . Subsequently, we acidified samples and blanks in a desiccator
147 containing 5 % HCl. Isotope signatures were measured on an EA-IRMS, a Flash EA 1112
148 coupled to a DeltaV advantage IRMS (Thermo Electron Instruments) with a single low
149 volume oxidation/reduction reactor (Carman & Fry 2002). Samples were calibrated against
150 VPDB and N_2 -Air with standards USGS40 and USGS41 (Qi et al. 2003) and all measurements
151 were corrected for blanks. Isotope values were expressed in δ notation with respect to VPDB
152 ($\delta^{13}\text{C}$) and air ($\delta^{15}\text{N}$): $\delta X (\text{‰}) = [(R_{\text{sample}}/R_{\text{standard}}) - 1] \times 10^3$, where X is ^{13}C or ^{15}N and R is the
153 isotope ratio (Post 2002).

154 **Transmission electron microscopy (TEM) and scanning transmission electron**
155 **microscopy energy dispersive x-ray (STEM-EDX) analysis.** *Sabatieria* and *Desmodora*, from
156 the seep sediment core, were imaged with TEM to check for symbionts or visible S
157 detoxification structures. Subsequently, we conducted STEM-EDX analysis to determine the

158 chemical composition of internal structures. Nematodes were handled following Van Gaever
159 et al. (2009b).

160 **Data analysis.** Individual nematode size measurements (length, width, length/width and
161 biomass) were compared among cores using Kruskal-Wallis tests, followed by nonparametric
162 pairwise comparisons using Behrens-Fisher tests with the R package npmc (Munzel &
163 Hothorn 2001, Helms & Munzel 2008). Nematode size measurements were averaged per
164 core and depth layer as geometric means corrected for data skewness (Middelburg et al.
165 1997, Soetaert et al. 2009). We performed multi-dimensional scaling (MDS) analysis on
166 standardized nematode genus abundances to compare genus composition between cores.
167 Diversity indices were Ln (\log_e)-transformed to highlight differences. We examined feeding
168 ecology based on (1) $\delta^{13}\text{C}$ and $\delta^{15}\text{N}$ of *Desmodora*, *Sabatieria* and “Mix”; and (2) buccal
169 morphology of all genera following the classification of Wieser (1952), which assigns genera
170 to one of 4 feeding types: selective deposit-feeder (1A), non-selective deposit-feeder (1B),
171 epistrate feeder (2A) and predator/scavenger (2B). Isotope signatures were compared
172 between *Sabatieria*, *Desmodora* and “Mix” using 1-way ANOVA, followed by post-hoc Tukey
173 HSD tests. Trophic diversity was computed as the reciprocal of the trophic index (Heip et al.
174 1985). Spearman-rank correlations were computed between distance from the seep site and
175 (1) genus diversity indices, (2) trophic diversity, and (3) stable isotope signatures. We
176 performed univariate statistical analyses using R (R Development Core Team 2010), and
177 multivariate analyses and computation of diversity indices in Primer v6 (Clarke & Gorley
178 2006).

179

RESULTS

180

Pore-water geochemistry

181 Fig. 2 shows concentration-depth profiles for H₂S, SO₄²⁻, CH₄ and TA in pore-water from all
182 cores. From the 4 cores, only the seep sediment core showed a clear decrease in SO₄²⁻ with
183 depth, accompanied by a peak in H₂S (up to 22 mM) and an increase in CH₄ and TA as high as
184 1000 μM and 33.7 meq l⁻¹ respectively. We observed very little change in SO₄²⁻ in the core
185 taken 2 m from the seep site. However, H₂S, CH₄ and TA were enriched in the deeper
186 sediment layers, relative to seawater,. Concentrations of all of these species in cores
187 collected 5 and 10 m from the seep site were similar to seawater concentrations and varied
188 little with depth.

189 **Meiofaunal community structure**

190 Meiofaunal densities were highest in the core taken 2 m from the seep site (3228.8 ind. 10
191 cm⁻²). Although densities in the seep sediment core (794.8 ind. 10 cm⁻²) and in the core
192 taken at 5 m distance (825.3 ind. 10 cm⁻²) were considerably lower, they were still elevated
193 compared to those collected 10 (227.7 ind. 10 cm⁻²), 100 (436.1 ind. 10 cm⁻²) and 1100 m
194 (424.3 ind. 10 cm⁻²) from the seep site (Fig. 3). Nematodes were the most abundant (88.7 –
195 94.5 %) in all cores (Table 2). Meiofaunal densities in the seep sediment core below 1 cm,
196 decreased sharply (Fig. 2). In comparison, densities in the core taken 2 m from the seep site
197 decreased more gradually with depth. Meiofauna in the 2 cores retrieved farthest from seep
198 influence penetrated deepest in the sediment.

199 **Nematode size**

200 Overall, total nematode biomass in the top 5 cm of the seep sediment core was
201 almost 10x higher than that in the core taken 1100 m away (Fig. 3). Individual nematode size
202 measurements (i.e. length, width, and biomass) differed significantly among cores (p <
203 0.001; Fig. 4) and peaked in the seep sediment core. Also nematode length/width ratios

204 varied significantly among cores ($p < 0.001$), with lowest ratios in the seep sediment core
205 (Fig. 4C). *S. vasicola* and *S. punctata*, which dominated the seep sediment core, were on
206 average 2416.5 ± 396.5 ($n = 42$) and 1130.8 ± 463.1 ($n = 33$) μm long respectively.

207 **Nematode community structure**

208 Nematode genus composition varied little among cores (Fig. 5, Table 3). *Sabatieria*
209 dominated all samples, except at 2 m from the seep site, where *Rhabdocoma* (23 %)
210 prevailed. All diversity indices correlated positively with distance from the seep site (Fig. 6),
211 but these correlations were significant only for N_0 and EG(100) (N_0 : $r = 0.93$, $p = 0.008$ and
212 EG(100): $r = 0.81$, $p = 0.049$). *Desmodora* was only abundant (i.e. $\geq 1\%$ of total) in cores
213 within 5 m off the seep (Table 3).

214 **Nematode feeding ecology**

215 $\delta^{13}\text{C}$ ranged between -40.7 ‰ and -21.3 ‰, and $\delta^{15}\text{N}$ varied between 0.9 and 15.3 ‰
216 (Fig. 7). $\delta^{13}\text{C}$ ($r = 0.34$, $p = 0.14$) and $\delta^{15}\text{N}$ ($r = 0.24$, $p = 0.28$) became heavier with increasing
217 distance from the seep site, though the correlations were not significant. No clear pattern
218 emerged when plotting stable isotope signatures vs. sediment depth (Fig. 7). “Mix” ($\delta^{13}\text{C}$: -
219 31.2 ± 4.9 ‰, $\delta^{15}\text{N}$: 7.11 ± 3.9 ‰) was significantly more enriched in ^{13}C ($p = 0.02$) and ^{15}N (p
220 $= 0.02$) than *Desmodora* ($\delta^{13}\text{C}$: -38.5 ± 2.0 ‰, $\delta^{15}\text{N}$: 4.6 ± 2.2 ‰). *Sabatieria* ($\delta^{13}\text{C}$: -36.3 ± 2.4
221 ‰, $\delta^{15}\text{N}$: 6.9 ± 1.5 ‰) and *Desmodora* displayed similar isotope values ($\delta^{13}\text{C}$: $p = 0.67$, $\delta^{15}\text{N}$:
222 $p = 0.43$). Based on buccal morphology, deposit-feeders (1A + 1B) dominated all cores (data
223 not shown), although trophic diversity increased with increasing distance from the seep site
224 ($r = 0.70$, $p = 0.12$), and leveled off at 10 m distance.

225 **TEM and STEM-EDX**

226 TEM revealed several, but mostly disintegrated bacteria bordering the cuticle of *Desmodora*
227 (Fig. 9). Additionally, electron-lucent structures were observed near the cuticle (Fig. 9B).
228 STEM-EDX analysis showed these contained trace amounts of sulphur. We observed no
229 symbionts or detoxification structures in *Sabatieria*.

230 DISCUSSION

231 CH₄ seepage and spatial variability in pore-water geochemistry

232 Elevated pore-water CH₄ levels in the Darwin MV seep sediment core indicated a CH₄ flux
233 from below the sediment surface, corroborating the gas escape from the seep sediments
234 during sampling. However, CH₄ concentrations dropped from 1 mM down to <0.001 mM
235 over a 10-m distance, suggesting focused flow. Pore-fluid analyses indicated some anaerobic
236 consumption by microbes (i.e. anaerobic oxidation of methane or AOM): SO₄²⁻ decreased
237 rapidly with depth in the seep site pore-fluids, accompanied by an increase in TA and
238 elevated H₂S concentrations (Reeburgh, 1976, Boetius et al. 2000, Knittel & Boetius 2009).
239 The relatively small enrichments in H₂S, CH₄ and TA in the core taken 2 m from the seep site,
240 suggest AOM presence here as well, but likely concentrated at depths exceeding the core
241 length. The constancy in the concentrations of SO₄²⁻, TA, H₂S and CH₄ with depth in the cores
242 taken at 5 and 10 m distance, suggest an absence of AOM. The high spatial variability in CH₄
243 flow at the Darwin MV illustrates the difficulty in taking replicate samples for pore-water
244 geochemistry and associated fauna at seeps.

245 Impact of pore-water geochemistry on meiofaunal distribution and tolerance to high H₂S levels

246 At the Darwin MV, meiofaunal densities were much higher in and immediately near
247 the seep site (2 m) compared to the sites showing no sign of seep influence in terms of pore-
248 water geochemistry. Accordingly, Vanreusel et al. (2010) showed elevated meiofaunal

249 standing stock in seep compared to non-seep sediments for several other seep systems. The
250 seep sediment core had high H₂S content (up to 22 mM), as shown for several other seeps
251 (Barry et al. 1997, Levin et al. 2003, Sahling et al. 2002). These high H₂S levels impacted the
252 vertical distribution in the sediment, in that the proportion of meiofauna confined to the
253 sediment surface was highest in this core. Tolerance of high H₂S levels was genus (and
254 species) specific. *Sabatieria* and *Desmodora*, which dominated the seep sediment core, were
255 more tolerant to high H₂S than genera absent from this core.

256 In sulphidic environments, bacterial symbionts can help to detoxify H₂S (Ott et al.
257 2004). In bathyal oxygen minimum zone sediments, *Desmodora masira* had ectosymbionts
258 (Bernhard et al. 2000). Although in our study, TEM cross-sections paralleled the annuli (in
259 contrast to Bernhard et al. 2000), the low and irregular bacterial appearance implies that
260 *Desmodora* from the seep sediment core did not harbour ectosymbionts. TEM showed
261 electron-lucent structures near the cuticle resembling the sulphur inclusions described by
262 Thiermann et al. (2000), but STEM-EDX analysis only detected traces of sulphur. However,
263 elemental sulphur is known to leach from vesicles during chemical fixation, dehydration, and
264 resin infiltration of biological samples, which may explain the low sulphur content (Lechaire
265 et al. 2006). Increased body length is another adaptation to sulphidic conditions, and
266 enables a fast migration between anoxic, sulphidic, and oxic, H₂S-free sediments
267 (Schratzberger et al. 2004, Levin 2005). Accordingly, *S. punctata*, and *S. vasicola*, which
268 dominated the seep sediment core, were amongst the longest nematodes in this study.

269 **Meiofaunal and nematode community structure**

270 Meiofaunal density patterns were mainly driven by the dominant taxon, i.e. the nematodes.
271 Nematodes dominate most seep habitats (Shirayama & Ohta 1990, Robinson et al. 2004, Van

272 Gaever et al. 2009a, Van Gaever et al. 2009c), although some habitats are dominated by
273 copepods (Van Gaever et al. 2006). In the Darwin MV seep sediment core, meiofauna-sized
274 polychaetes were subdominant, similar to the REGAB mussel beds (Van Gaever et al. 2009a).

275 Nematode genus composition clearly differed between cores with and without CH₄
276 flow. Thus, CH₄ flow affected not only densities and biomass, but also composition. Genus
277 diversity was lowest in the seep sediment core and increased in cores farther from the seep
278 site, as shown in previous studies (Van Gaever et al. 2009a,c). *Desmodora* and *Sabatieria*
279 also dominated the REGAB seep in the Gulf of Guinea (Van Gaever et al. 2009a), although in
280 association with different habitats: the REGAB samples originated from clam and mussel
281 fields with low H₂S content (<0.1 μM; Olu-Le Roy et al. 2009). *S. vasicola* and *S. punctata*,
282 which dominated the Darwin MV seep sediment core, also occur in shallow waters (Vitiello
283 1970, Jensen et al. 1992, Franco et al. 2008). Accordingly, the dominant species at the
284 REGAB seep (*S. mortenseni*), the Arctic Håkon Mosby MV (*Halomonhystera disjuncta*) (Van
285 Gaever et al. 2006), and the Nordic Nyegga seep (*Terschellingia longicaudata*) (Van Gaever
286 et al. 2009c) inhabit shallow waters as well. The presence of these species in both shallow
287 waters and at a deep-sea seep suggests a possible connection between these habitats,
288 rather than between deep-sea seeps (Van Gaever et al. 2009c).

289 **Feeding ecology**

290 δ¹³C values suggest thiotrophic C is part of the nematode diet up to 10 m from the seep site.
291 Except for “Mix” in sediment layer 4-6 cm, which displays a δ¹³C of -21.3 ‰, all δ¹³C were
292 less than -28 ‰. Organic matter produced through sulphur-oxidation has an average δ¹³C of
293 -30 ‰ (RubisCO I) or -11 ‰ (RubisCO II), depending on the Rubisco enzyme involved
294 (Robinson & Cavanaugh 1995). In comparison, photosynthetic C is characterized by δ¹³C

295 between -18 and -28 ‰ (Stewart et al. 2005), and CH₄-derived C is more depleted in ¹³C
296 ($\delta^{13}\text{C} < -50 \text{ ‰}$) (Levin & Michener 2002). Since we did not sample potential C sources for
297 stable isotope analysis, we cannot estimate their relative contribution to the nematode diet.
298 Nonetheless, a decrease in thiotrophic (RubisCO I) and an increase in photosynthetic C in the
299 nematode diet farther from the seep site are implied by (1) the thicker hemipelagic
300 sediment veneer on top of the cores, suggesting a higher availability of photosynthetic C, (2)
301 an increase in trophic diversity, and (3) heavier $\delta^{13}\text{C}$.

302 Spies et al. (1983) and Van Gaever et al. (2006, 2009b) reported direct nematode
303 consumption of sulphur-oxidisers. These bacteria live at the interface between oxic and
304 anoxic sediments, where H₂S levels are $\leq 1 \mu\text{M}$ (Robertson & Kuenen 2006, Preisler et al.
305 2007). We doubt these bacteria inhabited the seep sediments given the absence of bacterial
306 mats and the high H₂S levels at greater depth. In the core collected 2 m from the seep site,
307 we observed no net SO₄²⁻ production, expected in the presence of sulphur-oxidisers.
308 Nematodes can indirectly consume sulphur-oxidisers by assimilating dissolved organic
309 matter (DOM) released upon bacterial lysis. Jensen (1987) suggested thiobiotic nematodes
310 feed, at least partially, on DOM. However, further evidence is needed to support this
311 hypothesis. Stable isotope signatures suggest different feeding strategies for *Sabatieria* and
312 *Desmodora* compared with the bulk nematode community, which may explain their success.
313 As with other seeps (Vanreusel et al. 2010), deposit-feeders dominated. Finally, although
314 this exploratory study hints at how meiofauna interacts with the seep environment, much
315 more, high-resolution research is required to understand their tolerance of sulphide, trophic
316 interactions, and dispersal capacities.

317 *Acknowledgements.* The research leading to these results has received funding from the European
318 Community's Seventh Framework Programme (FP7/2007-2013) under the HERMIONE project, grant agreement
319 n° 226354 and was supported by the FWO "cold seeps" project n° G034607. The authors are greatly indebted
320 to the crew and the captain of the *RRS James Cook* and the pilots of ROV *Isis* for their expertise and

321 professionalism. We also gratefully acknowledge M. Claeys for her assistance and the preparation of the TEM
322 photographs. Finally yet importantly, we greatly appreciated the comments of the editor, the reviewers, and
323 Lois Maignien.

324 LITERATURE CITED

- 325 Andrassy I (1956) The determination of volume and weight of nematodes. *Acta Zool Hung* 2:1-15
326 Barry JP, Kochevar RE, Baxter CH (1997) The influence of pore-water chemistry and physiology on the
327 distribution of vesicomid clams at cold seeps in Monterey Bay: implications for patterns of
328 chemosynthetic community organization. *Limnol Oceanogr* 42:318-328
329 Bernhard JM, Buck KR, Farmer MA, Bowser SS (2000) The Santa Barbara Basin is a symbiosis oasis.
330 *Nature* 403:77-80
331 Boetius A, Ravensschlag K, Schubert CJ, Rickert D, Widdel F, Gieseke A, Amann R, Jorgensen BB, Witte
332 U, Pfannkuche O (2000) A marine microbial consortium apparently mediating anaerobic
333 oxidation of methane. *Nature* 407:623-626
334 Carman KR, Fry B (2002) Small-sample methods for delta $\delta^{13}\text{C}$ and delta $\delta^{15}\text{N}$ analysis of the diets of
335 marsh meiofaunal species using natural-abundance and tracer-addition isotope techniques.
336 *Mar Ecol Prog Ser* 240:85-92
337 Clarke K, Gorley R (2006) PRIMER v6: User Manual/tutorial. Primer-E Ltd, Plymouth
338 Dando PR, Austen MC, Burke RA, Kendall MA, Kennicutt MC, Judd AG, Moore DC, O'Hara SCM,
339 Schmaljohann R, Southward AJ (1991) Ecology of a North Sea pockmark with an active
340 methane seep. *Mar Ecol Prog Ser* 70:49-63
341 Franco MA, Soetaert K, Van Oevelen D, Van Gansbeke D, Costa MJ, Vincx M, Vanaverbeke J (2008)
342 Density, vertical distribution and trophic responses of metazoan meiobenthos to
343 phytoplankton deposition in contrasting sediment types. *Mar Ecol Prog Ser* 358:51-62
344 Genio L, Johnson SB, Vrijenhoek RC, Cunha MR, Tyler PA, Kiel S, Little CTS (2008) New record of
345 "Bathymodiolus" mauritanicus Cosel 2002 from the Gulf of Cadiz (NE Atlantic) mud
346 volcanoes. *J Shellfish Res* 27:53-61
347 Grasshoff K, Ehrhardt M, Kremling K, Anderson L (1999) Methods of seawater analysis. Wiley-VCH,
348 Weinheim
349 Heip C, Vincx M, Vranken G (1985) The ecology of marine nematodes. *Oceanogr Mar Biol Annu Rev*
350 23:399-489
351 Helms J, Munzel U (2008) npmc: Nonparametric Multiple Comparisons. R package version 10-7
352 Hoehler T, Borowski W, Alperin M, Rodriguez N, Paull C (2000) Model, stable isotope and radiotracer
353 characterization of anaerobic methane oxidation in gas hydrate-bearing sediments of the
354 Blake ridge. *Proc Ocean Drilling Prog: Sci Results* 164:79-85
355 Ivanenkov V, Lyakhin Y (1978) Determination of total alkalinity in seawater. In: Methods of
356 hydrochemical investigations in the ocean. Nauka Publ. House, Moscow, p 110-114
357 Jensen P (1984) Measuring carbon content in nematodes. *Helgolander Meeresun* 38:83-86
358 Jensen P (1987) Feeding ecology of free-living aquatic nematodes. *Mar Ecol Prog Ser* 35:187-196
359 Jensen P, Aagaard I, Burke RA, Dando PR, Jorgensen NO, Kuijpers A, Laier T, Ohara SCM,
360 Schmaljohann R (1992) 'Bubbling Reefs' in the Kattegat: submarine landscapes of carbonate-
361 cemented rocks support a diverse ecosystem at methane seeps. *Mar Ecol Prog Ser* 83:103-
362 112
363 Knittel K, Boetius A (2009) Anaerobic oxidation of methane: progress with an unknown process. *Annu*
364 *Rev Microbiol* 63:311-334
365 Lamshead PJD, Boucher G (2003) Marine nematode deep-sea biodiversity - hyperdiverse or hype? *J*
366 *Biogeogr* 30:475-485
367 Lechaire JP, Frebourg G, Gaill F, Gros O (2006) In situ localization of sulphur in the thioautotrophic
368 symbiotic model *Lucina pectinata* (Gmelin, 1791) by cryo-EFTEM microanalysis. *Biol Cell*
369 98:163-170

370 Levin LA, Michener RH (2002) Isotopic evidence for chemosynthesis-based nutrition of
371 macrobenthos: The lightness of being at Pacific methane seeps. *Limnol Oceanogr* 47:1336-
372 1345

373 Levin LA, Ziebis W, Mendoza GF, Growney VA, Tryon MD, Brown KM, Mahn C, Gieskes JM, Rathburn
374 AE (2003) Spatial heterogeneity of macrofauna at northern California methane seeps:
375 influence of sulfide concentration and fluid flow. *Mar Ecol Prog Ser* 265:123-139

376 Levin LA (2005) Ecology of cold seep sediments: Interactions of fauna with flow, chemistry and
377 microbes. *Oceanogr Mar Biol Annu Rev* 43:1-46

378 Middelburg JJ, Soetaert K, Herman PMJ (1997) Empirical relationships for use in global diagenetic
379 models. *Deep-Sea Res I* 44:327-344

380 Munzel U, Hothorn LA (2001) A unified approach to simultaneous rank test procedures in the
381 unbalanced one-way layout. *Biom J* 43:553-569

382 Olu-Le Roy K, Lance S, Sibuet M, Henry P, FialaMedioni A, Dinert A (1997) Cold seep communities as
383 indicators of fluid expulsion patterns through mud volcanoes seaward of the Barbados
384 accretionary prism. *Deep-Sea Res I* 44:811-841

385 Olu-Le Roy K, Caprais JC, Galéron J, Causse R, von Cosel R, Budzinski H, Ménach KL, Roux CL, Levaché
386 D, Khripounoff A (2009) Influence of seep emission on the non-symbiont-bearing fauna and
387 vagrant species at an active giant pockmark in the Gulf of Guinea (Congo–Angola margin).
388 *Deep-Sea Res II* 56:2380-2393

389 Ott J, Bright M, Bulgheresi S (2004) Symbioses between marine nematodes and sulfur-oxidizing
390 chemoautotrophic bacteria. *Symbiosis* 36:103-126

391 Pinheiro LM, Ivanov MK, Sautkin A, Akhmanov G, Magalhaes VH, Volkonskaya A, Monteiro JH,
392 Somoza L, Gardner J, Hamouni N (2003) Mud volcanism in the Gulf of Cadiz: results from the
393 TTR-10 cruise. *Mar Geol* 195:131-151

394 Post DM (2002) Using stable isotopes to estimate trophic position: Models, methods, and
395 assumptions. *Ecology* 83:703-718

396 Preisler A, de Beer D, Lichtschlag A, Lavik G, Boetius A, Jorgensen BB (2007) Biological and chemical
397 sulfide oxidation in a *Beggiatoa* inhabited marine sediment. *Isme J* 1:341-353

398 Qi HP, Coplen TB, Geilmann H, Brand WA, Bohlke JK (2003) Two new organic reference materials $\delta^{13}\text{C}$
399 and $\delta^{15}\text{N}$ measurements and a new value for the $\delta^{13}\text{C}$ of NBS 22 oil. *Rapid Commun Mass*
400 *Spectrom* 17:2483-2487

401 R Development Core Team (2010) R: A language and environment for statistical computing. R
402 Foundation for Statistical Computing, Vienna, available at <http://www.R-project.org>

403 Reeburgh WS (1976) Methane consumption in Cariaco Trench waters and sediments. *Earth Planet Sc*
404 *Lett* 28:337-344

405 Reeburgh WS (2007) Oceanic methane biogeochemistry. *Chem Rev* 107:486-513

406 Robertson L, Kuenen J (2006) The Colorless Sulfur Bacteria. In: Dworkin M, Falkow S, Rosenberg E,
407 Schleifer K-H, Stackebrandt E (eds) *The Prokaryotes: ecophysiology and biochemistry*.
408 Springer, New York, p 985-1011

409 Robinson C, Bernhard J, Levin L, Mendoza G, Blanks J (2004) Surficial hydrocarbon seep infauna from
410 the Blake Ridge (Atlantic Ocean, 2150 m) and the Gulf of Mexico (690-2240 m). *Mar Ecol*
411 *25*:313-336

412 Robinson JL, Cavanaugh CM (1995) Rubisco in chemoautotrophic symbioses: Implications for the
413 interpretation of stable carbon isotope values. *Limnol Oceanogr* 40:1496-1502

414 Sahling H, Rickert D, Lee RW, Linke P, Suess E (2002) Macrofaunal community structure and sulfide
415 flux at gas hydrate deposits from the Cascadia convergent margin, NE Pacific. *Mar Ecol Prog*
416 *Ser* 231:121-138

417 Schratzberger M, Whomersley P, Warr K, Bolam SG, Rees HL (2004) Colonisation of various types of
418 sediment by estuarine nematodes via lateral infaunal migration: a laboratory study. *Mar Biol*
419 *145*:69-78

420 Seeberg-Elverfeldt J, Schlüter M, Feseker T, Kölling M (2005) Rhizon sampling of pore waters near the
421 sediment/water interface of aquatic systems. *Limnol Oceanogr- Meth* 3:361-371

- 422 Shirayama Y, Ohta S (1990) Meiofauna in a cold-seep community off Hatsushima, Central Japan. *J*
423 *Oceanogr* 46:118-124
- 424 Soetaert K, Franco M, Lampadariou N, Muthumbi A, Steyaert M, Vandepitte L, vanden Berghe E,
425 Vanaverbeke J (2009) Factors affecting nematode biomass, length and width from the shelf
426 to the deep sea. *Mar Ecol Prog Ser* 392:123-132
- 427 Somoza L, Diaz-del-Rio V, Leon R, Ivanov M, Fernandez-Puga MC, Gardner JM, Hernandez-Molina FJ,
428 Pinheiro LM, Rodero J, Lobato A, Maestro A, Vazquez JT, Medialdea T, Fernandez-Salas LM
429 (2003) Seabed morphology and hydrocarbon seepage in the Gulf of Cadiz mud volcano area:
430 acoustic imagery, multibeam and ultra-high resolution seismic data. *Mar Geol* 195:153-176
- 431 Spies R, DesMarais D (1983) Natural isotope study of trophic enrichment of marine benthic
432 communities by petroleum seepage. *Mar Biol* 73:67-71
- 433 Stewart FJ, Newton ILG, Cavanaugh CM (2005) Chemosynthetic endosymbioses: adaptations to oxic-
434 anoxic interfaces. *Trends Microbiol* 13:439-448
- 435 Thierman F, Vismann B, Giere O (2000) Sulphide tolerance of the marine nematode *Oncholaimus*
436 *campylocercoides* – a result of internal sulphur formation? *Mar Ecol Prog Ser* 193: 251-259
- 437 Thurber AR, Kröger K, Neira C, Wiklund H, Levin LA (2009) Stable isotope signatures and methane use
438 by New Zealand cold seep benthos. *Mar Geol* 272:260-269
- 439 Van Gaever S, Moodley L, de Beer D, Vanreusel A (2006) Meiobenthos at the Arctic Hakon Mosby
440 Mud Volcano, with a parental-caring nematode thriving in sulphide-rich sediments. *Mar Ecol*
441 *Prog Ser* 321:143-155
- 442 Van Gaever S, Galéron J, Sibuet M, Vanreusel A (2009a) Deep-sea habitat heterogeneity influence on
443 meiofaunal communities in the Gulf of Guinea. *Deep-Sea Res II* 56:2259-2269
- 444 Van Gaever S, Moodley L, Pasotti F, Houtekamer M, Middelburg JJ, Danovaro R, Vanreusel A (2009b)
445 Trophic specialisation of metazoan meiofauna at the Hakon Mosby Mud Volcano: fatty acid
446 biomarker isotope evidence. *Mar Biol* 156:1289-1296
- 447 Van Gaever S, Olu-Le Roy K, Derycke S, Vanreusel A (2009c) Metazoan meiofaunal communities at
448 cold seeps along the Norwegian margin: influence of habitat heterogeneity and evidence for
449 connection with shallow-water habitats. *Deep-Sea Res I* 56:772-785
- 450 Van Rensbergen P, Depreiter D, Pannemans B, Moerkerke G, Van Rooij D, Marsset B, Akhmanov G,
451 Blinova V, Ivanov M, Rachidi M, Magalhaes V, Pinheiro L, Cunha M, Henriot J-P (2005) The El
452 Arraiche mud volcano field at the Moroccan Atlantic slope, Gulf of Cadiz. *Mar Geol* 219:1-17
- 453 Vanreusel A, Andersen AC, Boetius A, Connelly D, Cunha MR, Decker C, Hilario A, Kormas KA,
454 Maignien L, Olu K, Pachiadaki M, Ritt B, Rodrigues CF, Sarrazin J, Tyler PA, Van Gaever S,
455 Vanneste H (2009) Biodiversity of cold seep ecosystems along the European margins.
456 *Oceanography* 22:110-127
- 457 Vanreusel A, De Groote A, Gollner S, Bright M (2010) Ecology and biogeography of free-living
458 nematodes associated with chemosynthetic environments in the deep sea: a review. *Plos*
459 *One* 5:1-15
- 460 Vitiello P (1970) Nématodes libres marins des vases profondes du Golfe du Lion. II Chromadorida.
461 *Téthys* 2:449-500
- 462 Wieser W (1952) Die Beziehung zwischen Mundhöhlengestalt, Ernährungsweise und Vorkommen bei
463 freilebenden marinen Nematoden. Eine ökologisch-morphologische Studie. *Arkiv för Zoologi*
464 4:439-483

FIGURE CAPTIONS

- 467 Fig. 1. (A) Bathymetric map of the Darwin MV with the core locations on the MV indicated
468 (©NOC 2009) (B) Schematic representation of the sampling strategy. PUC1: push core 1,

469 sampled for pore-water geochemistry and meiofaunal community analyses; PUC2: push core
470 2, sampled for pore-water CH₄ concentration, porosity and nematode stable isotope
471 signatures; MC: megacorer, sampled for meiofaunal community analyses

472 Fig. 2. Vertical pore-water profiles of H₂S, SO₄²⁻, CH₄ and TA, and sedimentary densities of
473 nematodes and other meiofaunal taxa in relation to distance from the Darwin MV seep site.
474 Vertical arrows indicate seawater values. Note the different scales on the graphs

475 Fig. 3. Total nematode densities and biomass in relation to distance from the Darwin MV
476 seep site (0-5 cm)

477 Fig. 4. Mean nematode (A) length, (B) width, (C) length/width and (D) biomass in function of
478 sediment depth (cm), in relation to distance from the Darwin MV seep site

479 Fig.5. MDS plot of standardized genera-abundance data in relation to distance from the
480 Darwin MV seep site. Numbers indicate sediment depth (cm). Contour plots were not drawn
481 for the cores collected at 100 and 1100 m from the seep site as these overlapped

482 Fig. 6. Ln-transformed diversity indices based on nematode genera abundances in relation to
483 distance from the Darwin MV seep site. N₀, N₁, N_{inf}: Hill's numbers; J': Pielou's evenness
484 number; H': Shannon-Wiener Diversity index; EG(100): expected number of genera for
485 n=100

486 Fig. 7. *Desmodora* (Des), *Sabatieria* (Sab) and "Mix" (A) C and (B) N isotope signatures in
487 relation to distance from the Darwin MV seep site. At 10-m distance, no δ¹³C was available
488 for 0-2 cm due to the low amount of C, making the isotope value unreliable. Colours
489 represent sediment layers (white: 0-2 cm, grey: 2-4 cm, black: 4-6 cm)

490 Fig. 8. Nematode trophic diversity in relation to distance from the Darwin MV seep site (0-5
491 cm)

492 Fig. 9. TEM micrograph of a cross-section of *Desmodora* from the Darwin MV seep sediment
493 core. (A) Overview, (B) Detail showing bacteria associated with the cuticle. The white arrow
494 points to empty structures, possibly containing S prior to ethanol dehydration. Ba: bacterial
495 cell

496

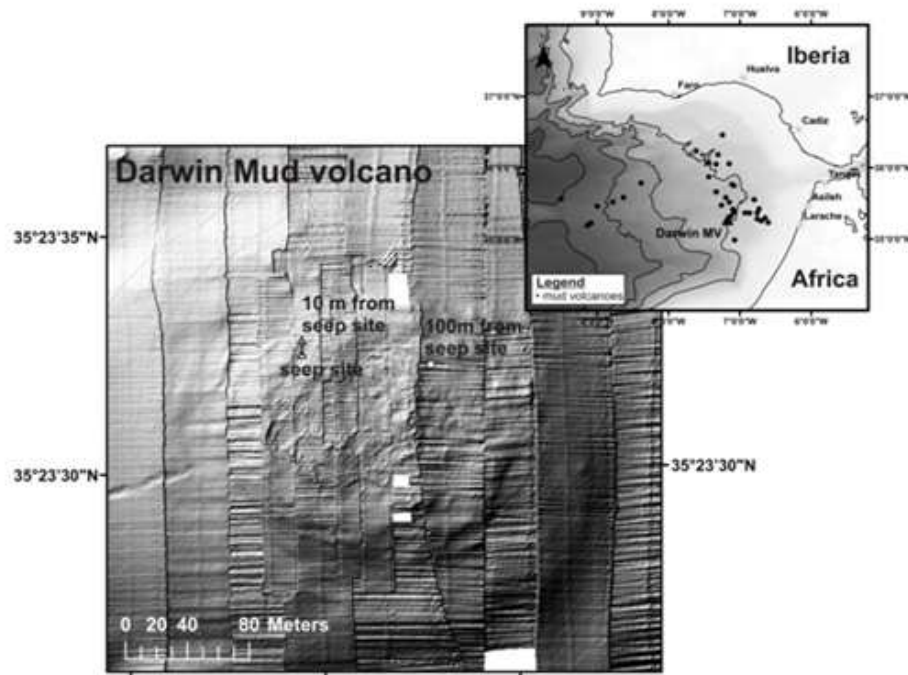
497

FIGURES

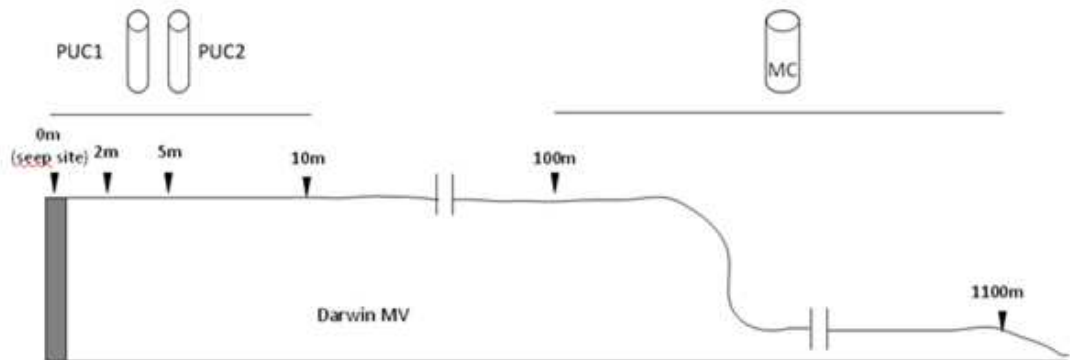
498 Fig. 1

499

A



B



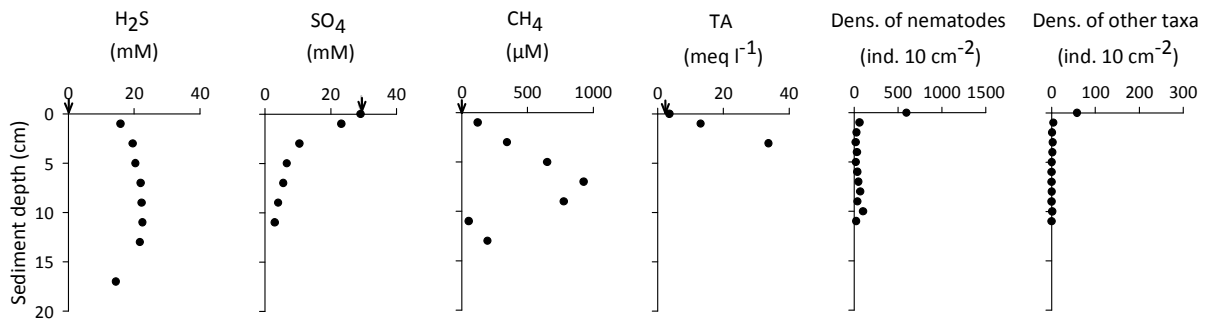
500

501

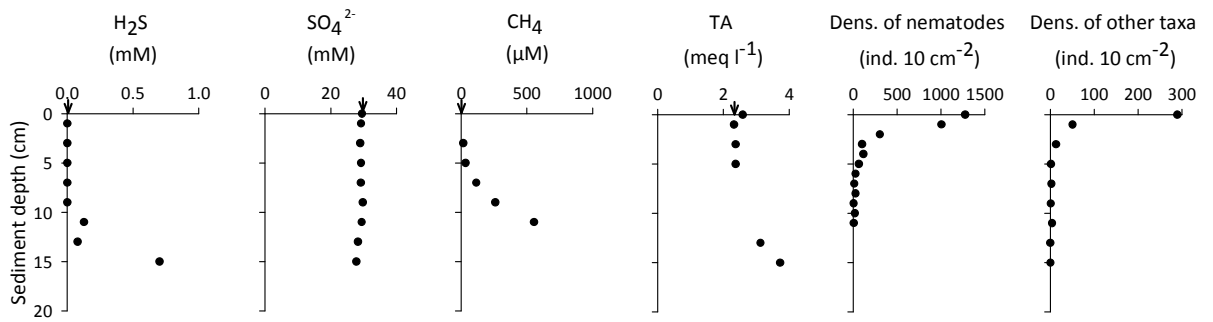
502

503 Fig. 2

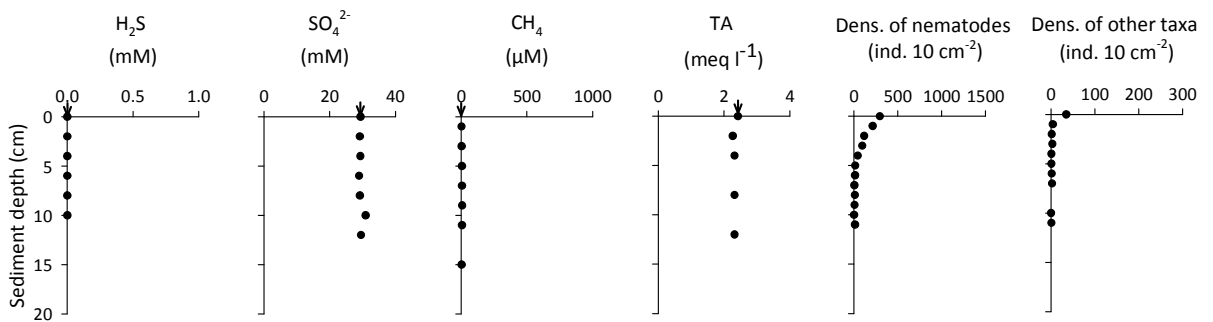
Seep sediment



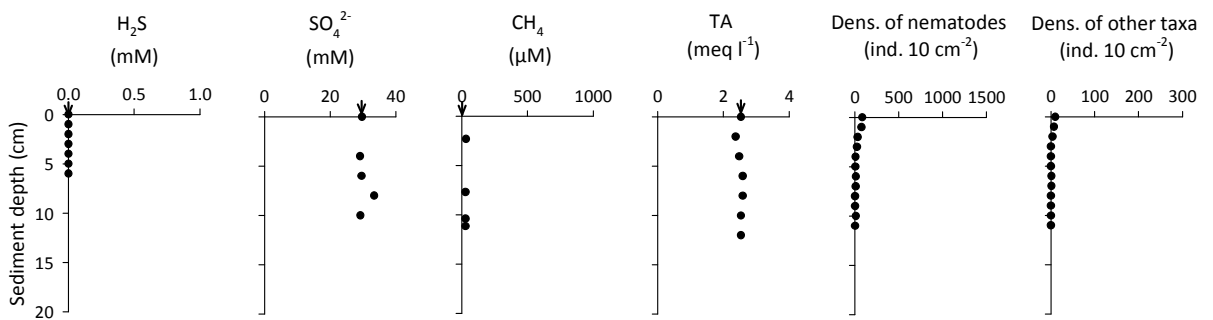
2 m from seep site



5 m from seep site



10 m from seep site

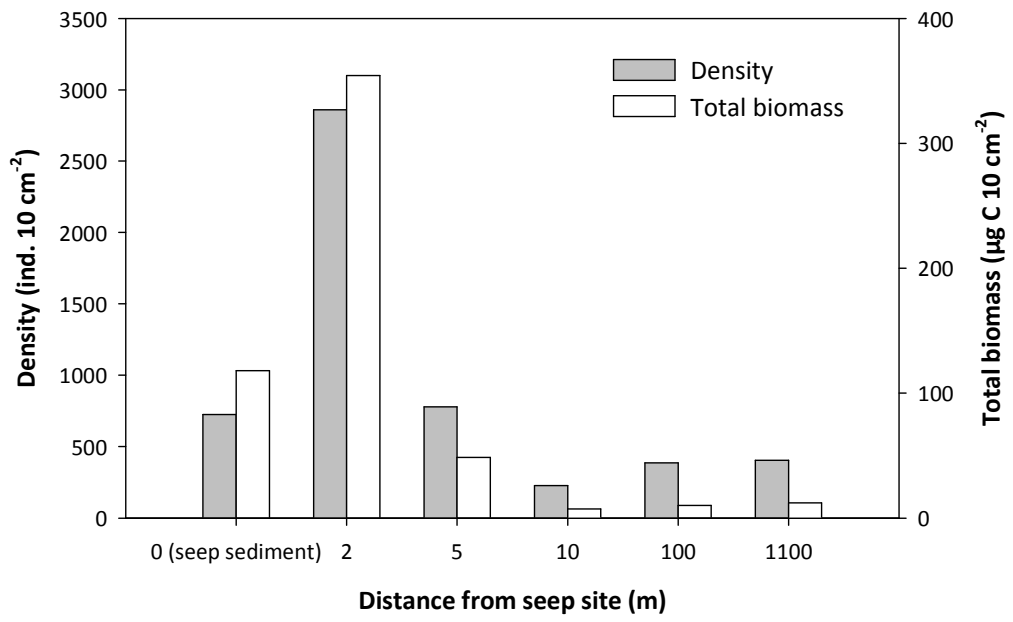


504

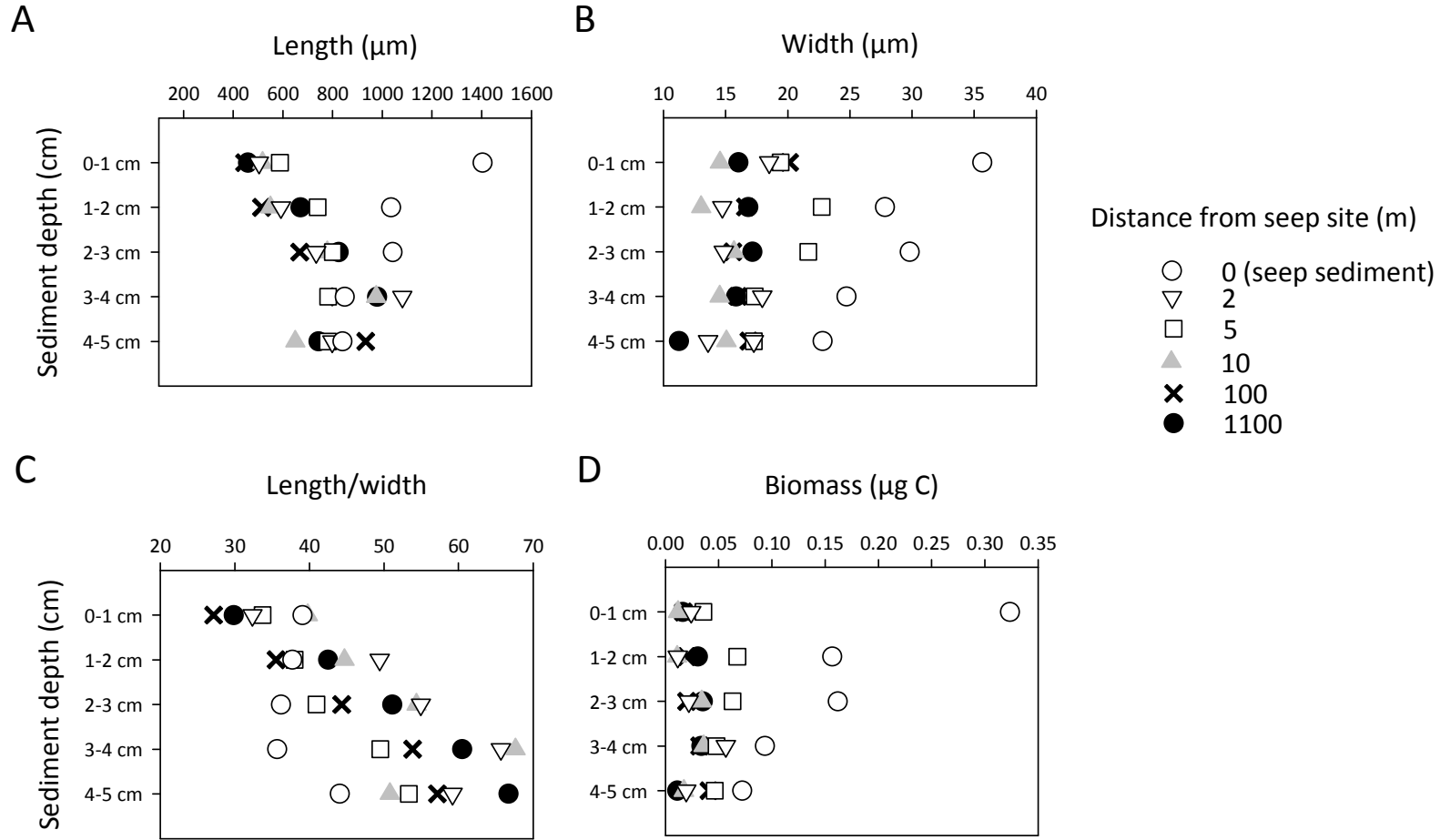
505

506 Fig. 3

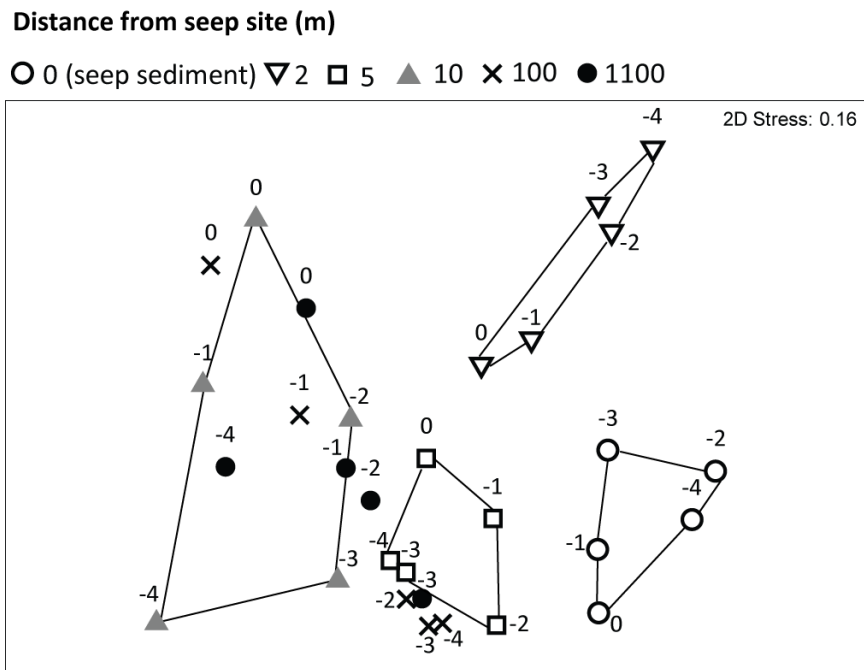
507



508

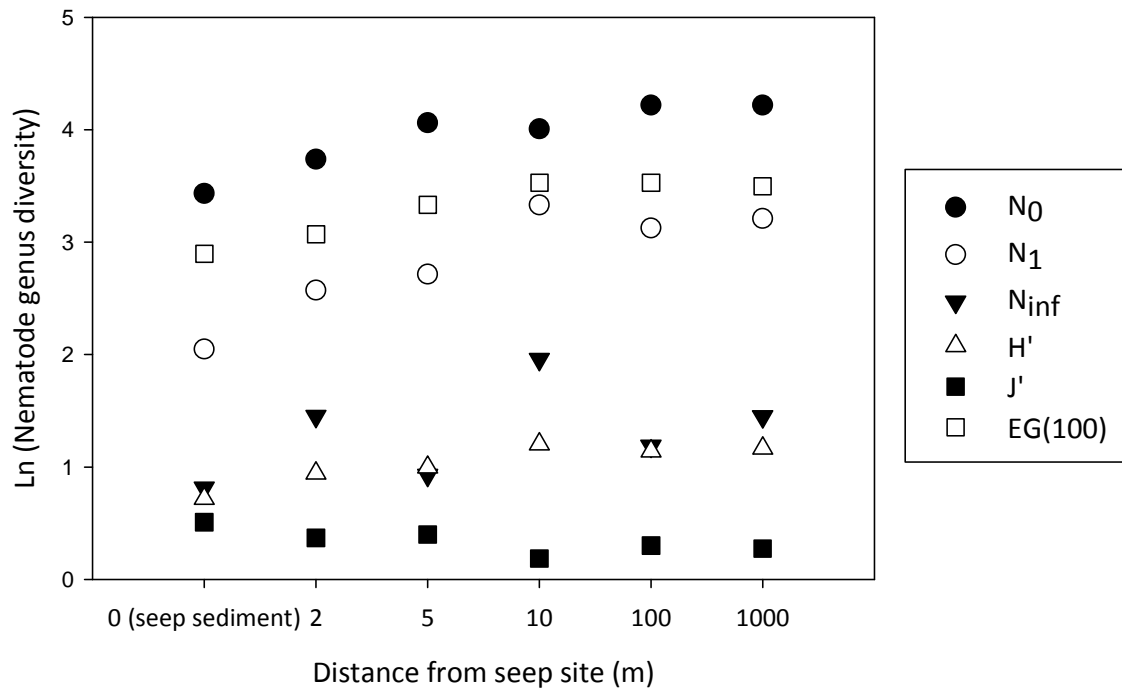


511 Fig. 5



512

513 Fig. 6

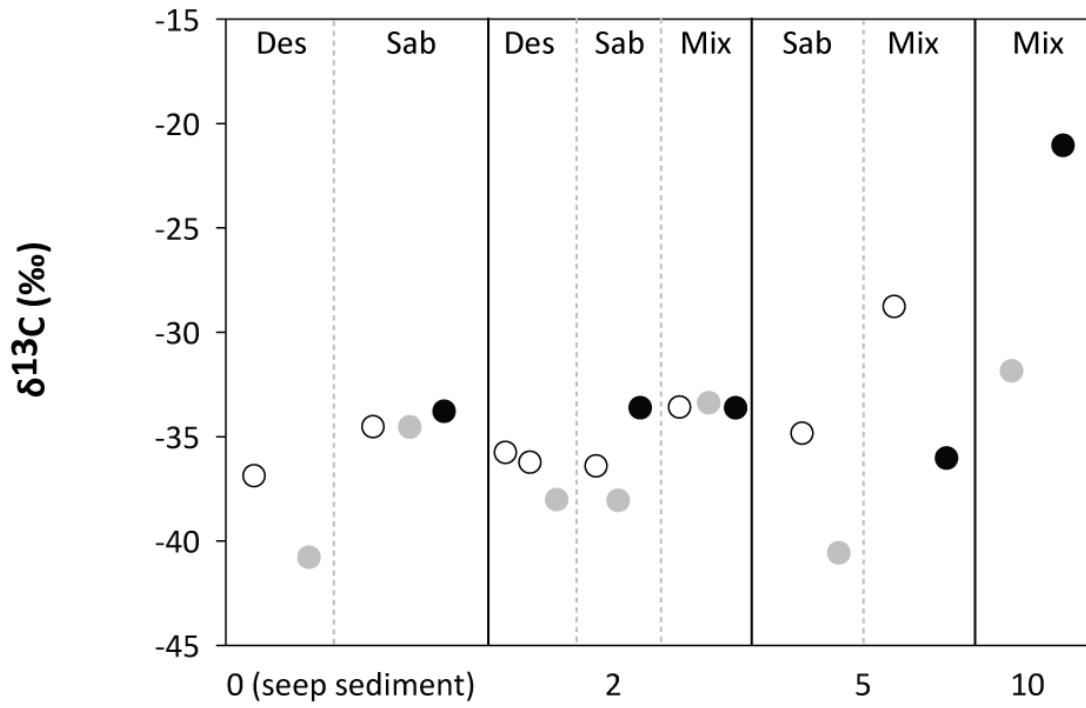


514

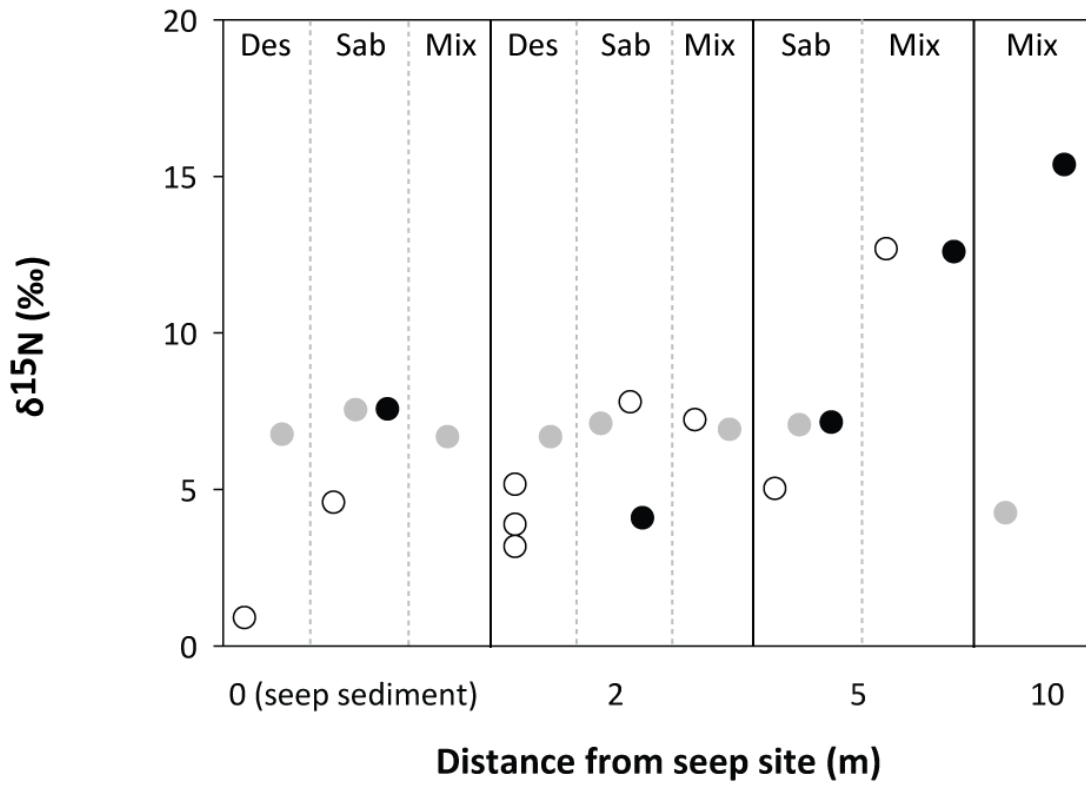
515

516

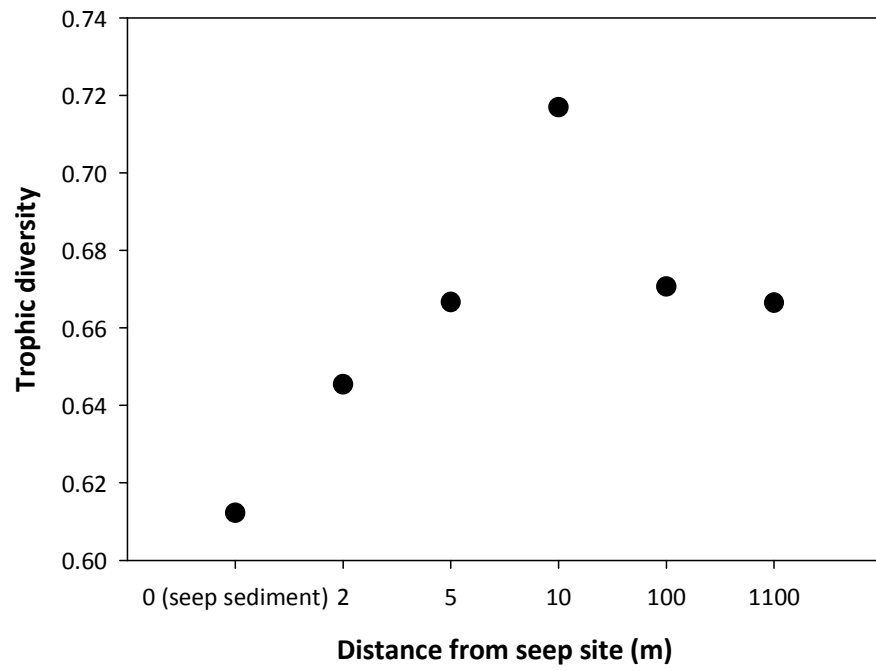
A



B

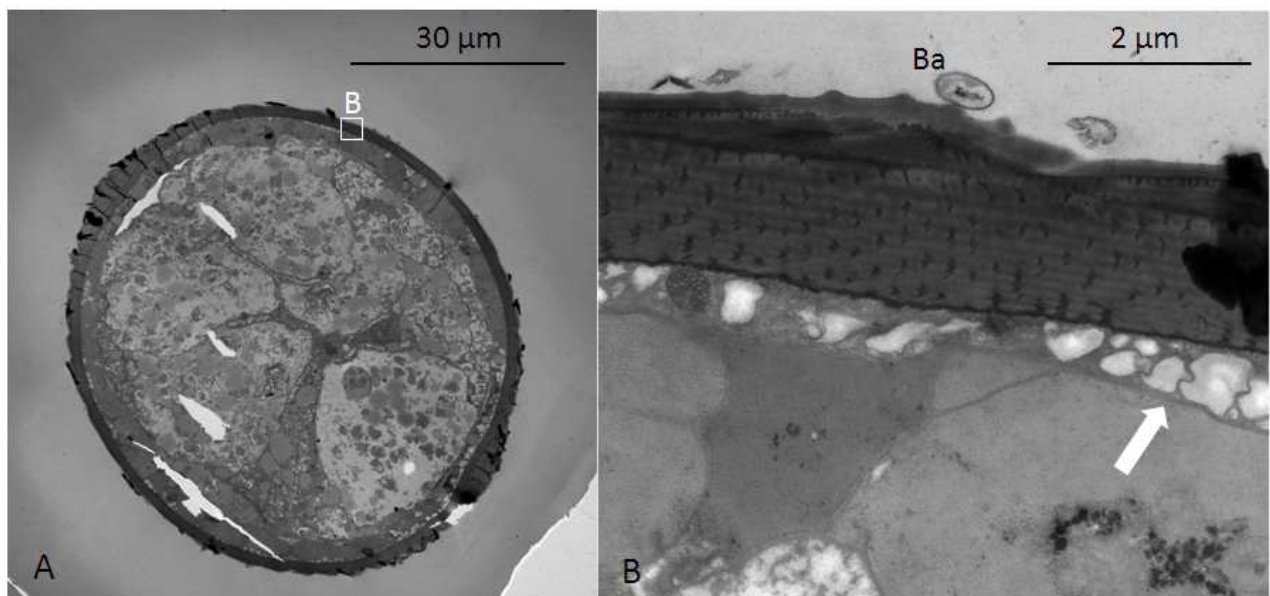


519 Fig. 8



520

521 Fig. 9



522

523

TABLE CAPTIONS

524 Table 1. Parameters of the sediment core locations in relation to distance from the Darwin MV
525 seep site. PUC: push core, MC: megacore

526 Table 2. Meiofaunal densities in relation to distance from the Darwin MV seep site (0-5 cm)

527 Table 3. Relative abundances of the most abundant nematode genera ($\geq 1\%$) in relation to
528 distance from the Darwin MV seep site (0-5 cm)

529 Table 4. Relative abundances of *Sabatieria* species in relation to distance from the Darwin MV
530 seep site (0-5 cm)

531 **TABLES**

532 Table 1

Distance from seep site (m)	Position	Height hemipelagic layer (% core length)	Gear	N° of cores	Analyses
0 (seep sediment)	35°23.539'N, 7°11.508'W	0	PUC	2	PUC1: meiofaunal community structure and pore-water geochemistry PUC2: porosity, pore-water CH ₄ concentration and nematode stable isotopes
2	35°23.543'N, 7°11.506'W	22-33	PUC	2	PUC1: meiofaunal community structure and pore-water geochemistry PUC2: porosity, pore-water CH ₄ concentration and nematode stable isotopes
5	35°23.543'N, 7°11.509'W	53-63	PUC	2	PUC1: meiofaunal community structure and pore-water geochemistry PUC2: porosity, pore-water CH ₄ concentration and nematode stable isotopes
10	35°23.547'N, 7°11.511'W	71	PUC	2	PUC1: meiofaunal community structure and pore-water geochemistry PUC2: porosity, pore-water CH ₄ concentration and nematode stable isotopes
100	35°23.537'N, 7°11.454'W	100	MC	1	meiofaunal community structure
1100	35°23.965'N, 7°11.121'W	100	MC	1	meiofaunal community structure

Taxon	Distance from seep site (m)					
	0 (seep sediment)	2	5	10	100	1100
Density (ind. 10 cm⁻²)						
Amphipoda		0.8				
Bivalvia	2.0		1.2		0.1	
Cladocera				0.4		
Cnidaria		4.3		0.8		0.3
Copepoda	7.84	121.9	12.5	3.9	16.9	7.7
Cumacea				0.4	0.3	0.1
Gastrotricha	0.4		1.6			
Halacaroidea	4.7	2.7	0.4			
Holothuroidea		1.2			7.7	0.4
Hydrozoa	0.4					
Isopoda		3.9	0.4	0.4	0.9	0.1
Kinorhyncha	0.8			0.4		
Nauplii	9.8	154.8	9.4	4.7	11.1	2.5
Nematoda	725.0	2860.1	779.5	227.7	387.9	405.4
Oligochaeta	0.8	9.8	5.1			0.1
Ostracoda		0.8	1.6		1.1	0.4
Polychaeta	42.7	54.5	7.1	9.8	8.7	5.9
Tanaidacea		3.5	0.8	0.4		
Tardigrada		8.6	5.9		1.5	1.2
Total	794.4	3226.9	825.3	248.4	436.1	424.3

534

535

536 Table 3

537

		Distance from seep site (m)									
0 (seep sediment)		2	5	10	100	1100					
<i>Sabatieria</i>	44.2	<i>Rhabdocoma</i>	23.5	<i>Sabatieria</i>	39.3	<i>Sabatieria</i>	14.1	<i>Sabatieria</i>	30.3	<i>Sabatieria</i>	23.6
<i>Desmodora</i>	19.2	<i>Amphimonhystrella</i>	18.6	<i>Thalassomonhystera</i>	7.8	<i>Molgolaimus</i>	11.4	<i>Thalassomonhystera</i>	8.6	<i>Thalassomonhystera</i>	9.6
<i>Ethmolaimidae n.gen.</i>	8.2	<i>Sabatieria</i>	14.4	<i>Desmodora</i>	5.6	<i>Daptonema</i>	6.4	<i>Hopperia</i>	6.0	<i>Acantholaimus</i>	7.0
<i>Desmoscolex</i>	6.0	<i>Ethmolaimidae n.gen.</i>	8.0	<i>Acantholaimus</i>	4.4	<i>Acantholaimus</i>	6.0	<i>Acantholaimus</i>	5.0	<i>Amphimonhystrella</i>	5.7
<i>Tricoma</i>	2.5	<i>Daptonema</i>	6.3	<i>Molgolaimus</i>	4.0	<i>Thalassomonhystera</i>	5.7	<i>Molgolaimus</i>	3.4	<i>Theristus</i>	5.7
<i>Amphimonhystrella</i>	2.5	<i>Desmodora</i>	5.3	<i>Microlaimus</i>	3.8	<i>Halalaimus</i>	4.4	<i>Diplopeltula</i>	2.8	<i>Halalaimus</i>	4.1
<i>Linhomeus</i>	2.2	<i>Tricoma</i>	3.8	<i>Halalaimus</i>	3.8	<i>Theristus</i>	4.4	<i>Halalaimus</i>	2.6	<i>Hopperia</i>	4.1
<i>Comesa</i>	1.6	<i>Linhomeus</i>	1.9	<i>Aegialolaimus</i>	2.0	<i>Amphimonhystrella</i>	4.0	<i>Leptolaimus</i>	2.4	<i>Molgolaimus</i>	2.7
<i>Thalassomonhystera</i>	1.1	<i>Molgolaimus</i>	1.7	<i>Hopperia</i>	2.0	<i>Syringolaimus</i>	3.4	<i>Amphimonhystrella</i>	2.2	<i>Leptolaimus</i>	2.5
<i>Cyartonema</i>	1.1	<i>Thalassomonhystera</i>	1.5	<i>Amphimonhystrella</i>	2.0	<i>Sphaerolaimus</i>	3.0	<i>Greefiella</i>	1.7	<i>Diplopeltula</i>	2.3
		<i>Theristus</i>	1.5	<i>Syringolaimus</i>	1.8	<i>Nemanema</i>	2.7	<i>Microlaimus</i>	1.7	<i>Aegialolaimus</i>	2.1
		<i>Microlaimus</i>	1.3	<i>Desmoscolex</i>	1.6	<i>Leptolaimus</i>	2.4	<i>Theristus</i>	1.7	<i>Syringolaimus</i>	2.1
		<i>Leptolaimoides</i>	1.1	<i>Tricoma</i>	1.5	<i>Microlaimus</i>	2.4	<i>Desmoscolex</i>	1.5	<i>Cervonema</i>	1.8
				<i>Monhystrella</i>	1.1	<i>Halichoanolaimus</i>	2.4	<i>Halichoanolaimus</i>	1.5	<i>Daptonema</i>	1.8
				<i>Leptolaimus</i>	1.1	<i>Aegialolaimus</i>	2.4	<i>Cervonema</i>	1.4	<i>Neochromadora</i>	1.8
				<i>Nyctonema</i>	1.1	<i>Oxystomina</i>	1.7	<i>Neochromadora</i>	1.4	<i>Doliolaimus</i>	1.4
				<i>Rhabdocoma</i>	1.1	<i>Neochromadora</i>	1.7	<i>Aegialolaimus</i>	1.2	<i>Oxystomina</i>	1.4
						<i>Rhabdocoma</i>	1.7	<i>Monhystrella</i>	1.2	<i>Desmoscolex</i>	1.2
						<i>Linhystera</i>	1.3	<i>Oxystomina</i>	1.2	<i>Leptolaimoides</i>	1.2
						<i>Leptolaimoides</i>	1.3	<i>Campylaimus</i>	1.0	<i>Microlaimus</i>	1.2
						<i>Hopperia</i>	1.3	<i>Linhystera</i>	1.0		
						<i>Prototricoma</i>	1.0	<i>Omicronema</i>	1.0		
						<i>Metadesmolaimus</i>	1.0	<i>Paracomesoma</i>	1.0		
						<i>Linhomeus</i>	1.0	<i>Prototricoma</i>	1.0		
								<i>Syringolaimus</i>	1.0		

538

539

540 Table 4

Distance from seep site (m)											
0 (seep sediment)		2		5		10		100		1100	
Species	%	Species	%	Species	%	Species	%	Species	%	Species	%
<i>S. vasicola</i>	28.5	<i>S. bitumen</i>	38.0	<i>S. bitumen</i>	40.7	<i>S. bitumen</i>	39.5	<i>S. ornata</i>	10.5	<i>S. stekhoveni</i>	51.6
<i>S. punctata</i>	20.8	<i>S. ornata</i>	34.7	<i>S. aff. breviseta</i>	16.3	<i>S. stekhoveni</i>	19.7	<i>S. bitumen</i>	10.2	<i>S. aff. breviseta</i>	9.5
<i>S. stekhoveni</i>	18.2	<i>S. propisinna</i>	17.5	<i>S. propisinna</i>	16.3	<i>S. ornata</i>	15.8	<i>S. demani</i>	7.2	<i>S. propisinna</i>	7.9
<i>S. ornata</i>	10.1	<i>S. stekhoveni</i>	9.7	<i>S. demani</i>	12.2	<i>S. propisinna</i>	13.2	<i>S. stekhoveni</i>	5.2	<i>S. conicauda</i>	6.7
<i>S. aff. breviseta</i>	8.3			<i>S. stekhoveni</i>	11.7	<i>S. demani</i>	11.8	<i>S. aff. breviseta</i>	3.4	<i>S. demani</i>	5.7
<i>S. conicauda</i>	4.7			<i>S. ornata</i>	2.7			<i>S. conicauda</i>	2.7	<i>S. lawsi</i>	5.7
<i>S. demani</i>	4.7							<i>S. punctata</i>	2.0	<i>S. ornata</i>	5.7
										<i>S. punctata</i>	4.3
										<i>S. vasicola</i>	2.9

541

542